LU TP 95-34
December 1995

Structure Functions and General Final State Properties in the Linked Dipole Chain Model

B. Andersson [1], G. Gustafson [2], H. Kharraziha[3], J. Samuelsson [4]

Department of Theoretical Physics
Lund University
Sölvegatan 14A
S-223 62 Lund, Sweden

Abstract

We have in an earlier paper, [1], presented a generalization, the Linked Dipole Chain Model LDC, of the model developed by Ciafaloni-Catani-Fiorani-Marchesini, [2], to decribe the structure functions and the states in Deep Inelastic Scattering events. In this paper we would like to present an investigation of a set of general features of the LDC Model, viz the behaviour of the structure functions (we will show how the result interpolates in a precise way in between the well-known DGLAP and BFKL approaches), the average bremsstrahlung emission in the states and finally a partitioning of the structure functions into three different channels: the "ordinary" parton-probe events, where all bremsstrahlung emissions are below the probe Q^2, the boson-gluon fusion events where the last splitting of the parton chains contain transverse momentum above Q^2, and the resolved Rutherford scattering events between the probe and the hadron (where the largest transverse momentum occur somewhere along the emission lines away from the ends).

[1]bo@thep.lu.se (internet)
[2]gosta@thep.lu.se(internet)
[3]hamid@thep.lu.se (internet)
[4]jim@thep.lu.se (internet)

1 Introduction

A major problem in Deep Inelastic Scattering (DIS) is to calculate the flux-factors of the available partons, ie the structure functions of the participating hadron. In a perturbative treatment of QCD this means the summation over a large amount of Feynman graphs relating the constituents, which occur on a certain "initial" scale, to those of the "final" scale, determined by the properties of the probe.

It is not necessary to know all the radiation in the states in order to be able to calculate (this change in) the flux factors. It is perfectly feasible to subdivide the emissions into two sets, "the main emissions", which we conventionally will refer to as the Initial State Bremsstrahlung (ISB) set, and "the remainder" (the Final State Bremsstrahlung, FSB), which is possible to emit in case the ISB is already provided. (In the calculations of the cross-sections the FSB is treated as the contributions from the radiative corrections to the main ISB emissions).

It is possible to make any choice of the ISB set for a particular configuration as long as the FSB can be emitted from this set *in accordance with the coherence conditions of QCD.* (It is, of course, useful to chose the ISB so that the later FSB emissions do not disturb the original configurations very much by recoils and kinematics). For a particular choice of the ISB it is, however, necessary to calculate the corresponding radiative corrections to these real emissions. In the perturbative QCD cascades the results of such calculations exponentiate (at least for the leading contributions, eg in the Leading Log Approximation,LLA) and are known as the corresponding Sudakov factors. It should be recognized, however, that if one changes the ISB set, eg by including some of the "earlier" ISB gluons into the FSB set, then it is also necessary to change the corresponding radiative corrections.

The Sudakov factors obtained by the exponentiation of the radiative corrections can often be interpreted in a probabilistic language. Then they correspond to the probability to not emit anything inside the phase space regions where it should have been dynamically allowed. The perturbative QCD cascades are in general formulated as stochastical processes. There is then an (inclusive) density of emissions in phase space dn, which will lead to an inclusive probability $d\mathcal{P}$ to emit a particular set of partons (the coherence conditions in the QCD radiation are taken into account by introducing an ordering of the process). The semi-inclusive probability to emit just those partons and to emit nothing inside the remaining region, Ω, (allowed by coherence, ie the ordering, and energy-momentum conservation) is then given by the formula

$$d\mathcal{P}\exp(-\int_\Omega dn) \tag{1}$$

The exponential factor is just the Sudakov factor, whether it is obtained by calculating the radiative corrections or by general probability arguments. The main point is, of course, that the radiative corrections to a given process often contains the same (inclusive) emission density dn as the "real" emissions.

In conclusion, although the inclusive emission density is the same at any bremsstrahlung vertex, it is necessary to "correct" with the proper Sudakov, depending upon the choice of the ISB gluons. In this way the resulting sum over all the contributions corresponding to the structure functions will be the same.

In an earlier paper, [1], we have presented a generalization and simplification of the model for the states in DIS, which has been developed by Ciafaloni, Catani, Marchesini and Fiorani (the CCFM Model), [2]. In the Linked Dipole Chain (LDC) Model there is a (small) change in the choice of the ISB set of gluons, as compared to the CCFM Model. While the set chosen in the CCFM Model can be described as the most general one possible, if one includes the QCD coherence conditions ("angular ordering") and request energy-momentum conservation at each emission vertex, the set chosen in the LDC Model is restricted to a (large) subset. The emissions which are in this way excluded from the initial state radiation, are instead included in the final state radiation.

In this way we obtain in the LDC Model that, [1]

I The Final State Bremsstrahlung (FSB) can be treated as the emission from a set of color dipoles, spanned by the chosen gluons in the ISB set. Therefore the FSB can be treated directly by means of the Lund Dipole Cascade Model (the DCM), which is implemented in the Monte Carlo simulation program ARIADNE, [3].

II The probabilities (in particular the radiative corrections) for the ISB set of states chosen in the LDC Model are simpler than the results for the CCFM Model. The stochastical process obtained is further explicitly "local" (Markovian) and symmetric with respect to emissions from the hadron end and the probe end. In this way the predictions of the LDC can be easily implemented into Monte Carlo simulation programs to study the particular ISB sets of the model.

III It is possible to incorporate into the formalism both the "ordinary" (perturbative) QCD parton interactions, the Boson-Gluon Fusion interactions and also the resolved (virtual) probe structure functions, including Rutherford interactions between the probe- and the hadron-ends. There is consequently in the LDC no cutoff (besides energy-momentum conservation) necessary for large transverse momenta in the ISB gluon emissions, at the same time as the gluonic bremsstrahlung in a well-defined way also cuts off small transverse momentum (Rutherford) scatterings.

Consequently the LDC Model and the DCM constitute a general method to treat all perturbative QCD interactions along the same lines, in terms of color dipole emissions. This approach directly fits into the final state hadronization model, ie the Lund String Fragmentation Model (as implemented in the Monte Carlo simulation program JETSET, [4])

Both the LDC and the CCFM models interpolate betwen the DGLAP (Dokshitzer-Gribov-Lipatov-Altarelli-Parisi) mechanism, which is relevant for large Q^2- and medium to small x_B-values and the BFKL (Balitsky-Fadin-Kuraev-Lipatov) mechanism, expected to be valid for medium Q^2 and very small x_B. We consider some properties of the models in section 2.

The intention of this note is to present some general results from the LDC Model. We are interested in the qualitative properties of the cascade, and therefore we restrict our study to a purely gluonic cascade without quarks, and we neglect nonsingular terms in the splitting function $P(z)$. We do however study the different results obtained for both a fixed and a running coupling α_s, for which significant differences are obtained. In subsection 4.1 we investigate the following properties by means of two calculational methods (the methods are presented in section 3 and correspond to different approaches to the basic equations):

A The behaviour of the structure functions for different (x_B, Q^2) (to be precise we treat emission from an incoming gluon at $x_{B0} = 1$ at a (small) initial virtuality Q_0^2 up to the probe at (x_B, Q^2); the methods will be extended to the other possible emission processes in future publications). We consider parametrizations of both the DGLAP type, $\propto \exp C\sqrt{\log(1/x_B)}$, and of the BFKL type $\propto x^{-\lambda}$ with C and λ possibly Q^2 dependent.

B The average "road" in the available phase space from (x_{B0}, Q_0^2) to (x_B, Q^2), together with the regions containing roads at most one standard deviation from the mean. At the same time we consider the density of the ISB gluon emission along the roads. We find that besides a small region "in the beginning" (about $3-4$ units in rapidity or $\log(1/x)$), which depends upon the starting-out conditions for the "undisturbed" hadronic wave-function constituents, there is a region in which the main road stays close to small $k_\perp$. Finally there is a region with a size depending upon the value of Q^2, ie the properties of the probe. The latter two regions correspond to contributions expected from a BFKL and a DGLAP treatment of the structure functions, respectively. The larger the total $\log(1/x)$ region is for a given $\log(Q^2)$ the more BFKL and vice versa for the DGLAP mechanism.

  Using our findings from A. and B. we present a new general parametrization of the structure functions for small x-values, which in a well-defined way interpolates between the DGLAP and BFKL contributions.

C The contributions to the structure functions from the different channels mentioned above for different (x_B, Q^2). In particular we investigate in some detail the regions where the DGLAP mechanism dominates, where the Boson-Gluon Fusion will provide essential contributions and where the (virtual) probe-hadron interactions contains large Rutherford contributions. In this way we exhibit the regions inside which a cut-off in the ISB gluon transverse momenta, $q_\perp^2$, by eg $q_\perp^2 < Q^2$ will be dangerous according to the LDC.

2 The LDC and the CCFM Models

2.1 Some properties of the CCFM Model

In order to describe the choice of the ISB set of gluon emissions in the CCFM Model we consider the fan diagram shown in Fig 1. This does not correspond to a single Feynman diagram but rather to a collection of such diagrams.

Along the main line from the incoming parton, denoted by the energy-momentum vector P, to the probe, with the vector $q = P_{probe}$, there is a set of initial state emissions called (q_j). Besides these gluons there is another set called (C_j) (the corresponding FSB) of emissions "in between" the q_j and q_{j+1}. There is further a set of "connector vectors", (k_j), between the q_j-emissions. Energy-momentum conservation is imposed for each q_j-emission (justified by chosing the q_j as

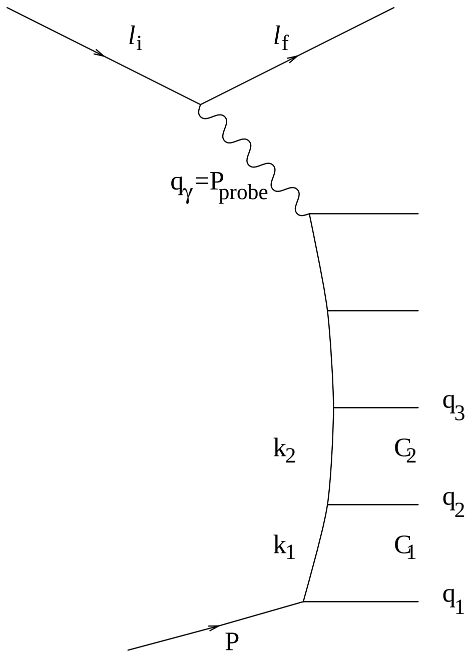

Figure 1: *A DIS fan diagram*

more "energetic", cf below, than the C_j-gluons):

$$k_j = P - \sum_{m=1}^{j} q_m \quad \text{ie} \quad k_j = k_{j-1} - q_j \tag{2}$$

All emissions are ordered in rapidity which (due to the relation between angle and rapidity) means *angular ordering* along the chain. The CCFM then pick the ISB (q_j) set from the set of all emissions as those which are not followed (in the rapidity ordering variable) by another one with a larger lightcone energy-momentum $q_+(= q_0 + q_\ell)$, ie in this way the q_j has larger "energy" than the rest. (We will later specify the meaning of the "longitudinal", ℓ, direction).

To be more precise we introduce the variables $(z_j, \vec{q}_{\perp j})$ with $k_{+j} = z_j k_{+(j-1)}$ and $\vec{k}_{\perp j} = \vec{k}_{\perp(j-1)} - \vec{q}_{\perp j}$. In the LLA the CCFM choice for the q_+ will imply $q_{+j} \ll q_{+(j-1)}$ which corresponds to an approximation of the splitting function $P(z) \simeq 1/z$ and the assumption that z is small enough so that $(1-z) \simeq 1$. Further the gluons in the sets (C_j) are in accordance with the LLA treated as soft enough so that the q-vectors can be taken on-shell and massless.

The corresponding propagator vectors k_j are, however, spacelike with the values $k_{+(j-1)} = q_{+j}/(1-z_j) \simeq q_{+j}$. The transverse momentum of the propagators $k_{\perp j}$ are dominated by the $q_\perp$-emissions in the neighbourhood (for a detailed discussion cf Ref [1]). One major kinematical constraint is that

$$k_{\perp j}^2 > z_j q_{\perp j}^2 \tag{3}$$

If this condition is not fulfilled then the "virtuality" of the propagator will in the LLA fulfil $|k^2| \gg k_\perp^2$, which implies strong suppression. Each step in the emission chain will in the CCFM Model be described by the weight

$$\bar{\alpha} \frac{dz_j}{z_j} \frac{dq_{\perp j}^2}{q_{\perp j}^2} \Delta_{ne}(z_j, k_{\perp j}, q_{\perp j}) \tag{4}$$

Here $\bar{\alpha} = 3\alpha_s/\pi$ is the effective coupling (including color factors) and Δ_{ne} is the so-called "non-eikonal formfactor" with

$$\Delta_{ne}(z_j, k_{\perp j}, q_{\perp j}) = \exp(-\bar{\alpha} \log(1/z_j) \log(k_{\perp j}^2 / z_j q_{\perp j}^2)) \tag{5}$$

The major result in the CCFM Model is this non-eikonal formfactor, corresponding to the radiative corrections for the choice of the ISB set defined above. We note in particular that due to the properties of the non-eikonal formfactor small values of z_j and $q_{\perp j}$ in Eq (4) are effectively cut-off in case we assume $k_\perp$ is finite.

2.2 The Properties of the LDC Model

In Ref [1] the results in Eqs (4) and (5) are analysed and reformulated. It is shown that the non-eikonal formfactor actually can be considered as an "ordinary" Sudakov formfactor, in the probability sense we described in section 1. The negative exponent is besides the $\bar{\alpha}$-factor a region excluded for gluon emission by the particular choice of the ISB $\{q_j\}$ in the CCFM Model.

In the LDC Model there is a restriction of the (q_j) states such that those gluons for which $q_{\perp j} < \min(k_{\perp j}, k_{\perp (j-1)})$ are included in the final state emission. This means that the remaining gluons satisfy the relation

$$q_{\perp j} \approx \max(k_{\perp j}, k_{\perp (j-1)}) \tag{6}$$

In this way we obtain in the LDC *that the weights in the q_j emissions are given by Eq (4) but with the non-eikonal formfactor Δ_{ne} exchanged for* 1. What is shown in Ref [1] is that *if we include into the FSB the gluons which in the CCFM belong to the IBS-set, but do not fulfil Eq (6), then the sum over the states containing such gluons, with the appropriate non-eikonal weights, will provide just the factor* 1.

This evidently corresponds to a major simplification and the weight in the LDC can be written solely in terms of the connectors (k_j). Integrating over the angle between $\vec{k}_{\perp j}$ and $\vec{k}_{\perp (j-1)}$ we obtain
(remember that $\vec{q}_{\perp j} = \vec{k}_{\perp (j-1)} - \vec{k}_{\perp j}$)

$$\int \frac{d\phi dk_{\perp j}^2}{q_{\perp j}^2} = \frac{dk_{\perp j}^2}{\max(k_{\perp j}^2, k_{\perp (j-1)}^2)} \cdot h(k_{\perp j}^2 / k_{\perp (j-1)}^2) \tag{7}$$

where the function $h(a)$ is given by

$$\begin{cases} h(a) = \frac{1}{1-a}\left[1 - \frac{2}{\pi} arctan\left(\frac{1+\sqrt{a}}{1-\sqrt{a}}\sqrt{\frac{2\sqrt{a}-1}{2\sqrt{a}+1}}\right)\theta(a - \frac{1}{4})\right] & ; 0 < a < 1 \\ h(a) = h(1/a) \end{cases} \tag{8}$$

In leading approximation $\log(k_{\perp j}^2 / k_{\perp (j-1)}^2)$ is not close to 0, and we have $h \approx 1$ which implies

$$\bar{\alpha}\frac{dz_j}{z_j}\int \frac{d\phi}{2\pi}\frac{dk_{\perp j}^2}{q_{\perp j}^2} \approx \begin{cases} \bar{\alpha} d\ln(1/z_j) d\kappa_j & \text{if } \kappa_j > \kappa_{j-1} \\ \bar{\alpha} d\ln(1/z_j) d\kappa_j \exp(\kappa_j - \kappa_{j-1}) & \text{otherwise} \end{cases} \tag{9}$$

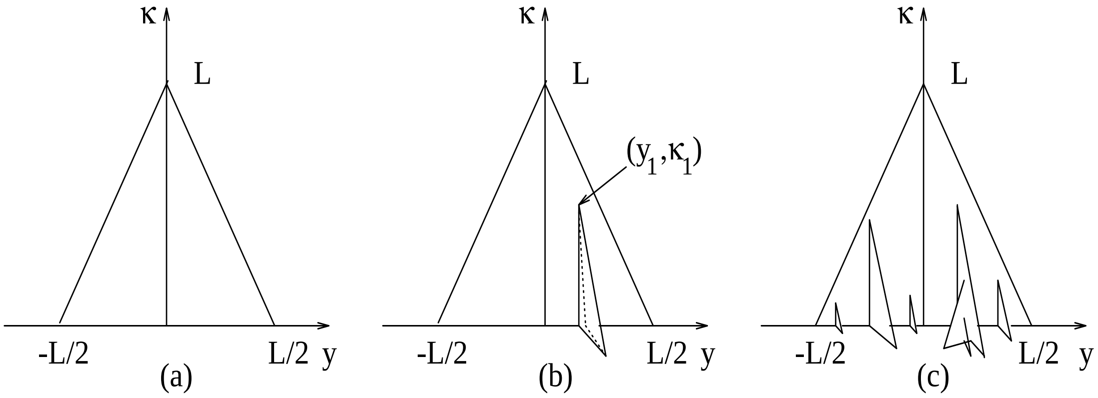

Figure 2: *The phase-space available for gluon emission from a dipole is a triangle in the (y,κ)-plane (a); in case one gluon is emitted at (y_1,κ_1) then the phase-space for a second (softer) gluon is the the area of the folded surface (below kappa$_1$) (b); each emitted gluon increases the phase-space for softer gluons and is represented by this many-facetted surface*

(the last factor stems from the requirement in Eq (6) and obviously corresponds to a "local" statement, ie a comparison of the sizes of two neighboring connector vectors).

Before we continue we will make a few comments on the time-like dipole cascades. We note that for a dipole bremsstrahlung emission (from eg a gluon-gluon (g_0, g_0') state) of a gluon g_1 with transverse momentum $q_{\perp 1}$ and rapidity y_1 the inclusive density dn_1 is in the LLA

$$dn_1((g_0,g_0') \to (g_0,g_1,g_0')) \equiv dn_1((g_0,g_1,g_0')) = \bar{\alpha} dy_1 \frac{dq_{\perp 1}^2}{q_{\perp 1}^2} \tag{10}$$

The phase space for such an emission from a dipole with mass W is in the dipole cms:

$$q_\perp \cosh(y) \leq W/2 \tag{11}$$

This relation can be conveniently approximated in the $(y, \log(q_\perp^2))$-plane, cf Fig 2, as the inside of a triangle

$$|y| \leq (L-\kappa)/2 \quad \text{with} \quad (L,\kappa) = (\log(W^2), \log(q_\perp^2)) \tag{12}$$

We note that in case we consider the corresponding inclusive density to emit two gluons at $(q_{\perp j}, y_j)$, $j = 1,2$ then the density is factorisable so that (this is shown to be good to about 99% all over phase space in Ref [6])

$$dn_2((g_0,g_0') \to (g_0,g_1,g_2,g_0')) = dn_1((g_0,g_1,g_0'))(dn_1((g_0,g_2,g_1)) + dn_1((g_1,g_2,g_0')) \tag{13}$$

in case $q_{\perp 1} > q_{\perp 2}$ (or else the indices have to be exchanged in Eq (13)). Thus "the original dipole" with (the basement) "length" L in accordance with Fig 2 is subdivided into two with the corresponding lengths $\pm y_1 + (L+\kappa_1)/2$. Each dipole can independently emit the gluon indexed 2 as shown in Fig 2. The requirement that $\kappa_2 < \kappa_1$ means that the two new dipole triangles are cut-off at the "height" κ_1. In this way we may define the notion of "virtuality" (as $\log(k_{\perp 1}^2) = \kappa_1$) for the newly produced dipoles.

In the Lund Dipole Cascade Model (DCM) this time-like cascade process is then continued in an obvious way into more and more gluon emissions with smaller and smaller dipoles. The

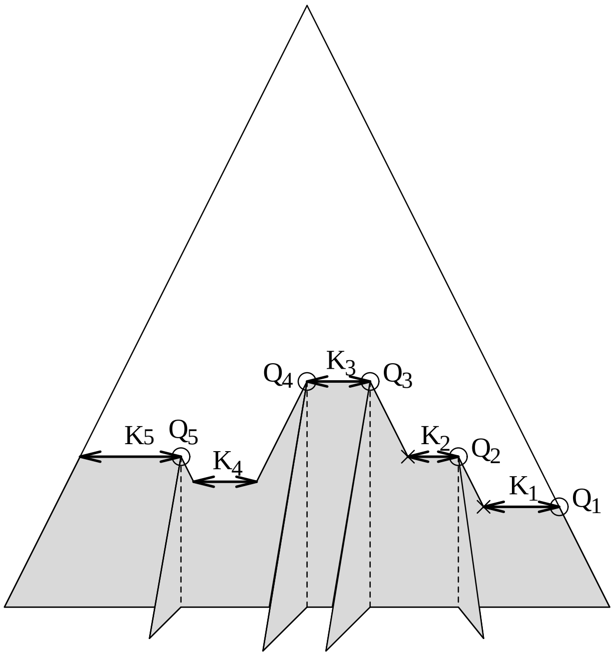

Figure 3: *A gluon-chain in the LDC Model described in the triangular phase-space. The extended folds correspond to on-the-mass-shell gluons and the arrows to the connector propagators*

main point is the ordering in $\kappa = \log(k_\perp^2)$ (which is the correspondence to the strong angular ordering, ie to the coherence conditions in the QCD radiation). This implies that any "new" emission at κ_j in a dipole is limited by the earlier "virtuality" of the dipole, ie $\kappa_{j-1} > \kappa_j$.

We also note that in the "geometry" of the triangular phase space, all points with a fixed value of $q_+ = q_{+j}$ ($q_- = q_{-j}$) are placed along lines parallell to the triangular side(s) because $\log(q_{\pm j}) = \pm y_j + \kappa_j/2$. In this way an on-shell (mass-less) gluon emission can be described either in terms of (q_{+j}, q_{-j}) or (what amounts to the crossing point of the two (logarithmic) "lightcone-lines") in terms of the coordinates (y_j, κ_j).

In order to interprete the results of the LDC and CCFM Models into the dipole phase space we note that there is in the fan diagram in Fig 1 in principle a large color "dipole". It is spanned between the incoming parton P (which we parametrize to be on the mass-shell with the positive lightcone energy-momentum P_+; in that way "the front lightcone line" corresponds to $\log(P_+)$) and the parton "kicked out" by the probe q (the probe is not on the mass-shell but provides the negative lightcone energy-momentum Q_- to the parton, ie the "backward lightcone line" corresponds to $-\log(Q_-)$). The essential ISB emissions, $\{q_j\}$, as well as the connector vectors, $\{k_j\}$, can be exhibited in this phase space triangle in the following way for the LDC:

LDCa. the q_j-vectors are onshell and massless and are therefore shown as extended triangular folds, just as we describe the emissions of the gluons in the time-like dipole cascade above

LDCb. the connector vectors k_j are not on the mass-shell but as we have mentioned before the component $k_{+j} = q_{+(j+1)}$ and (due to the necessary symmetry between the hadron and probe end) the component $k_{-j} = q_{-j}$. Finally the requirement in Eq (6) means that the transverse momentum $\log(k_{\perp j}^2)$ is fixed by the q_j emission (or vice versa). Therefore the k_j can be described by an extended line between the $q_{+(j+1)}$ and the q_{-j} at the appropriate height $\log(k_{\perp j}^2)$. (Note that in this way, cf also Eq (3), the "true" virtuality $-k_j^2 \simeq k_{\perp j}^2$)

Thus we obtain the picture in Fig 3 with a set of connected ISB dipoles spanned between the adjacent $\{q_j\}$ with the virtualities given by the corresponding connectors $\{\log(-k_j^2) \simeq \log(k_{\perp j}^2)\}$. The situation is obviously symmetric between the hadron and probe ends so that in Eq (9) we may interprete the splitting function z-pole either as the positive lightcone fraction $z = k_{+j}/k_{+(j-1)}(= q_{+(j+1)}/q_{+j})$ or the negative lightcone fraction $z \equiv z_- = k_{-j}/k_{-(j+1)}(= q_{-j}/q_{-(j+1)})$ (in case we would describe the process instead from the probe end).

In the CCFM Model more gluons are included in the essential ISB set. In particular when the requirement in Eq (6) is lifted the model no longer provides complete dipoles but also "parts of dipoles" as described in Ref [1]. We note one very important requirement, however. *In the FSB of the LDC Model (and this is the same for the CCFM Model) there can be no emission between the q_j and q_{j+1} with transverse momenta exceeding the virtuality of the connector $-k_j^2 \simeq k_{\perp j}^2$.*

The dynamical reason is that the gluon currents from the pair (q_j, q_{j+1}) due to the existence of the connector k_j "starts out" from two different space-time points. Therefore there is an "effective" (due to Lorentz contraction essentially transverse) distance between these emission points equal to $b \simeq 1/\sqrt{-k_j^2} \simeq 1/k_{\perp j}$. It is well-known that an "antenna" of the size b is not well-suited to emit radiation with the wave-length $\lambda < b$ (for smaller wave-length, ie larger transverse momenta, there will in general be a form-factor suppression). *The corresponding major result from the valiant CCFM Model calculations is that the dipole produced between q_j and q_{j+1} can emit no FSB bremsstrahlung with transverse momentum larger than the virtuality $-k_j^2 \simeq k_{\perp j}^2$.* There is a cancellation between the virtual and real corrections for the emission region above the transverse momentum $k_{\perp j}$ in between the gluons q_j and q_{j+1}.

2.3 The Different Channels in Deep Inelastic Scattering

We end this section with a subdivision into three different channels of the contributions from the dipole chains in the LDC. Firstly we note that the Bjorken x_B-variable is in this language $x_B = Q^2/2(pq) = Q_+Q_-/P_+Q_- = Q_+/P_+$. We have in Fig 4 shown both a description of the variables $\log(1/x_B)$ and $\log(Q^2)$, (note that the latter one occurs both as a rapidity region in the "big" dipole phase space triangle and as a measure of virtuality $\kappa_Q = \log(Q^2)$).

In Fig 4 we have shown three possible "chain-roads" and they correspond to, respectively

I a "normal" quark-parton model interaction, in which the largest virtuality along the chain is given by Q^2. The chain may after n emissions end anywhere along the line $\kappa_n < \log(Q^2) \equiv L_Q$ with a parton with $\prod^n z_j = x_B$. Depending upon the coordinate frame we consider (cf for more details Ref [1]) the parton will after the interaction with the probe end up at the point, denoted A at $(\log(1/x_B), \kappa = L_Q)$ (this would be in a Lorentz frame corresponding to the lepton-hadron cms) or at the point denoted E along the line with $\log(k_{-n}) = \log(Q_-)$ at the appropriate "incoming" virtuality κ_n (this is the

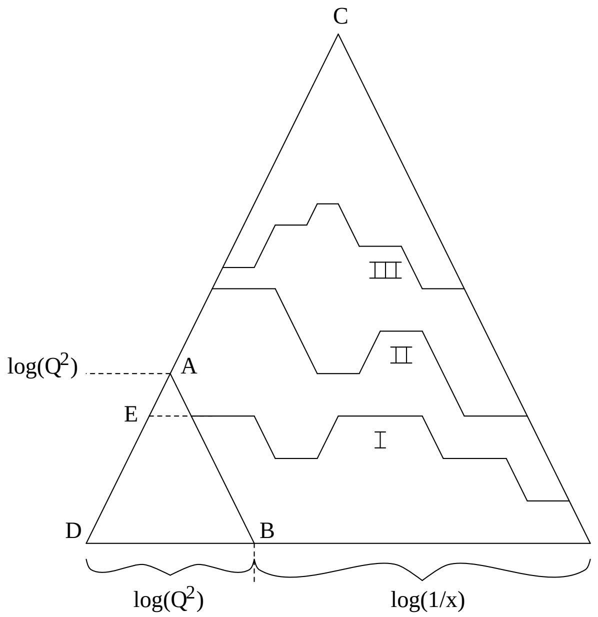

Figure 4: The different kinds of gluon chains. As the probe $Q_+ = xP_+$, cf text, the baseline rapidity region is divided into $(-\log(Q_-), \log(Q_+))$ and $(\log(Q_+), \log(P_+))$ with the marked out lengths $\log(Q^2)$ and $\log(1/x)$, respectively.

probe-hadron cms frame, where the transverse momentum of the kicked-out parton is provided solely by the cascade).

II a "Boson-Gluon Fusion" event, in which the (final) splitting transverse momentum variable exceeds the probe virtuality $\kappa_n (\simeq \log(q_{\perp n}^2)) > L_Q$. Then the final parton ends on the line $\log(Q_-)$ above the value L_Q, ie for $\kappa > L_Q$, due to this final (large virtuality) splitting. According to the way the structure function is defined we obtain from the weight factors of Eq (9) an extra "going-down" factor $Q^2/k_{\perp n}^2$. We call these events boson-gluon fusion events, although in the present study we have only gluons and no quarks, whereas in a real DIS event with γ, Z or W exchange the last parton in the chain has to be a quark.

III a Rutherford scattering between a remnant of the probe, which although it starts out at the probe virtuality L_Q splits up into a set of emissions $L_Q < \kappa_n < \kappa_{n-1} < \ldots < \kappa_{max}$ to "meet" the corresponding hadron remnant chain with $\kappa_1 < \kappa_2 < \ldots < \kappa_{max}$. In accordance with Eq (9) we will in this case obtain a factor (in the way we have defined it $\kappa_{max} = \log(k_{\perp max}^2)$ is the only maximum in transverse momentum along the chain)

$$\prod_1^n d\kappa_j \frac{Q^2 k_{\perp n}^2 k_{\perp(n-1)}^2 \cdots}{k_{\perp n}^2 k_{\perp(n-1)}^2 \cdots k_{\perp max}^2} = \prod_1^n d\kappa_j \frac{Q^2}{k_{\perp max}^2} \tag{14}$$

(We note that although the factor is described in the language of going from the hadron to the probe end, the result would be the same in case we would have used the opposite direction. We also note that this is a direct generalization of the going-down factor obtained in the case II described above).

The main point is, however, that in Eq (14) we obtain a factor $d\kappa_j = dk_{\perp j}^2/k_{\perp j}^2$ for all bremsstrahlung gluons but the factor $dk_{\perp max}^2/k_{\perp max}^4$ for the largest transverse momentum, which is characteristical for Rutherford scattering with $k_{\perp Ruth} = k_{\perp max}$. In Ref [1] it is shown that the correct Rutherford scattering behaviour occurs both when the propagator corresponds to a gluonic and when it is a quark(anti-quark) exchange.

Note that in this way (as we have mentioned before, [1], [7]) *the major momentum transfer in a chain diagram always corresponds to a Rutherford scattering* with (coherent) bremsstrahlung contributions describing both the "going-up" and "going-down" sides but all of them with $k_{\perp brems} < k_{\perp Ruth}$. *This means that the (largest) transverse momentum of the bremsstrahlung gluons always provide a lowest cut-off of a (possible) Rutherford scattering.*

3 Two Methods to Implement the LDC Model Equations

As we are interested in the qualitative features we are disregarding contributions from quarks, and we keep only the pole term $1/z$ in the gluonic splitting function. We have used two different ways, cf the subsections 3.1 and 3.2 to implement the LDC process. They are both based upon an integral equation.

It is useful to define "the non-integrated structure function", $\mathcal{F}$, instead of the structure function $F(x_B, Q^2)$ of the impinging hadron, by means of the equation

$$F(x_B, Q^2) = \int \frac{dk_\perp^2}{k_\perp^2} \mathcal{F}(\hat{\ell}, \kappa) \quad \text{with} \quad \hat{\ell} = \begin{cases} \log(1/x_B) \equiv \ell & \text{if } Q^2 > k_\perp^2 \\ \log(Q^2/x_B k_\perp^2) \cdot \frac{Q^2}{k_\perp^2} & \text{if } Q^2 < k_\perp^2 \end{cases} \tag{15}$$

In terms of the non-integrated structure function $\mathcal{F}$ we may write the following integral equation, corresponding to three contributions, $\mathcal{I}_j$:

$$\mathcal{F}(\ell, \kappa) = \sum_{j=1}^{3} \mathcal{I}_j \tag{16}$$

The contributions are in turn

- $\mathcal{I}_1$ the possibility $\mathcal{I}_1 = \bar{\alpha}$ to take a single step from the starting point ($\ell_0 \equiv \log(1/x_0), L_{Q_0} \equiv \log(Q_0^2)$) all the way to the final point ($\ell \equiv \log(1/x_B), \log(k_\perp^2) \equiv \kappa$) (this is a "boundary term"). (We often think of the parameter values ($\ell_0 = 0, L_{Q_0} = 0$), which define both the properties of the starting-point and the scale of the coupling.)

- $\mathcal{I}_2$ the possibility to be at a "point" (κ', ℓ') "below" κ, ie with ($L_{Q_0} < \kappa' \equiv \log(k_\perp'^2) < \kappa$ and $\ell_0 < \ell' \equiv \log(1/x') < \ell = \log(1/x_B)$), and to take the final step "upwards" in transverse momentum and "onwards" in ℓ. (This is the DGLAP mechanism.) We obtain

$$\mathcal{I}_2 = \int_{L_{Q_0}=0}^{\kappa} \bar{\alpha} d\kappa' \int_{\ell_0=0}^{\ell} d\ell' \mathcal{F}(\ell', \kappa') \cdot h(exp(\kappa - \kappa')) \tag{17}$$

  where $h \approx 1$ is defined in Eq (8).

$\mathcal{I}_3$ the possibility to be at a point κ' "above" κ and to take a step "downwards" to κ (note that this step is "upwards" in transverse momentum from the probe side and therefore we have to compensate with the change $\ell' \to \ell' + \kappa - \kappa'$, cf also Eq (9)):

$$\int_\kappa^\ell \bar{\alpha} d\kappa' \exp(\kappa - \kappa') \int_0^{\ell+\kappa-\kappa'} d\ell' \mathcal{F}(\ell', \kappa') \cdot h(exp(\kappa' - \kappa)) \tag{18}$$

We note that the factor h implies a suppression if we "stay" in the last step close to $\kappa \simeq \kappa'$, ie in case the emitted gluon transverse momentum is very small, $q_\perp \simeq 0$. This case has been treated extensively both inside the CCFM Model, [2] and the LDC, [1]. In CCFM it is noted that if the upper ℓ'-integral limit in Eq (18) is changed $\ell + \kappa - \kappa' \to \ell$ the integral equation obtained from Eqs (17) and (18) can be treated along the BFKL methods. After suitable rearrangements (with the non-eikonal form-factor regularising the singularity at $q_\perp = 0$) it also provides the well-known BFKL contribution.

Thus, in terms of the anomalous dimension equation, with the structure function $\mathcal{F}$ behaving like

$$\mathcal{F} \sim x^{-(N-1)} (k_\perp^2)^\gamma \tag{19}$$

one obtains in BFKL the result (written in the conventional form):

$$1 = \frac{\bar{\alpha}}{N-1} (g(\gamma) + g(1-\gamma)) \quad \text{with} \quad g(\gamma) = \psi(1) - \psi(\gamma) \tag{20}$$

In case the "correct" integral limit in $\mathcal{I}_3$ is retained there is a change in the argument of the second g-function $g(1-\gamma) \to g(N-\gamma)$. Therefore the change provides in the ordinary QCD language a contribution which is subleading in $\log(1/x)$, ie it is non-singular at the $(N-1)$-pole. We note, however, that this change at the same time provides a very large correction.

To see that we note that the two integral equations are symmetrical around $\gamma = 1/2$ and $\gamma = N/2$, respectively, and that the major contribution to the x-behaviour (the celebrated BFKL-exponent λ) comes for that value of N where there is "pinch" singularity in the inverse Mellin transform. For the case with $g(1-\gamma)$ this correspond to $\lambda \equiv N - 1 = 4\bar{\alpha}\log(2) \simeq 0.56$ (for $\alpha = 0.2$), but for the case with $g(N-\gamma)$ it is changed to $N - 1 \simeq 0.31$ (again for $\alpha = 0.2$).

If we introduce the restriction of the LDC Model in Eq (6) then the result will be similar to Eq (20) but the function g given for the BFKL case is slightly changed. The use of the precise LDC contribution provides another change to the BFKL result $N - 1 \simeq 0.41$ but we note that this change is smaller than the earlier one.

If we combine the experience obtained above from the different possible treatments of the small $q_\perp$-region with the arguments of Ref [1] that it is necessary to restrict the integration region in each z-step in order to conserve energy-momentum we may conclude:

- the results of taking all orders in transverse momentum fluctuations provide a rather stable result
- but there are large changes in the exponent λ describing the structure function from the different possible treatments of the small x-behaviour.

It has been known for a long time that there are corrections (principally of the order $\bar{\alpha}^2$ with a constant coupling) to the BFKL treatment. The fact that they are very large means that it is worthwhile trying to retain at least some of them. In this note we also will treat the consequences of introducing a running coupling.

3.1 A MC solution to the Integral Equation for LDC

We will here describe how we solve Eq (16) by first generating events evenly in an extended phase space, and afterwards multiply by appropriate weights. For all partons there is a cut $\kappa > 0$, corresponding to $p_\perp > \Lambda_{QCD}$. For running coupling constant we also have a cutoff such that $\bar{\alpha} \propto 1/\kappa$ for $\kappa > \kappa_{cut}$ ($= 2$ for the results presented below) and $\bar{\alpha} =$ constant for $\kappa < \kappa_{cut}$.

Suppose that we introduce the variables (for the case of a constant effective coupling $\bar{\alpha}$):

$$\begin{aligned} X &\equiv \sqrt{\bar{\alpha}} \log(Q/k_-) = \sqrt{\bar{\alpha}}(y - (\kappa - L_Q)/2) \\ Y &\equiv \sqrt{\bar{\alpha}} \log(k_+/Q) = \sqrt{\bar{\alpha}}(y + (\kappa - L_Q)/2) \end{aligned} \tag{21}$$

then the results of producing an ISB dipole (starting at some value (κ', y') and going to the point (κ, y)) is inclusively given by, cf Eq (9) (where we neglect the possible exponential "going-down" factor for the moment):

$$\bar{\alpha} dy d\kappa = dX dY \tag{22}$$

Further suppose that we introduce the following phase space, which is easily seen to be enlarged compared to the ordinary triangular dipole space:

$$\begin{aligned} 0 \leq X \leq a &\equiv \sqrt{\bar{\alpha}}(\log(Q^2) + \log(1/x)) \\ 0 \leq Y \leq b &\equiv \sqrt{\bar{\alpha}} \log(1/x) \end{aligned} \tag{23}$$

In order to exhibit the relationship between the variables (κ, y) in the triangular dipole phase space and the variables (X, Y) we show in Fig 5 a typical road (this time corresponding to a boson-gluon fusion event as described above).

We will now consider a stochastical process in the (X, Y)-plane, Eq (23), which is an approximation to the solution of the integral equation in Eq (16). Afterwards we will obtain the "correct" solution by introducing a weighting procedure for the steps.

The first step, which corresponds to emitting the first $q = q_1$-vector will always be placed along the right hand edge of the triangular phase space. In the LLA this corresponds to $q_{+1} \simeq P_+$, ie the step is along $Y = b$. In each of the following steps we will decide upon the position of the right end of the (next) propagator so that in the last step we end at the photon propagator. We then note that for every step there is a set of paths from "the starting-point" to the photon end. By our choice we will choose a subset of these paths. It is then necessary to weight every step by means of the available "remaining" possibilities, ie the remaining possible paths.

In the approximate process the weights for a path is given by $\prod dX_j dY_j$. Further we may introduce an ordering so that $a > X_1 > ... > X_n = 0$ and $b = Y_1 > ... > Y_n = 0$. This means

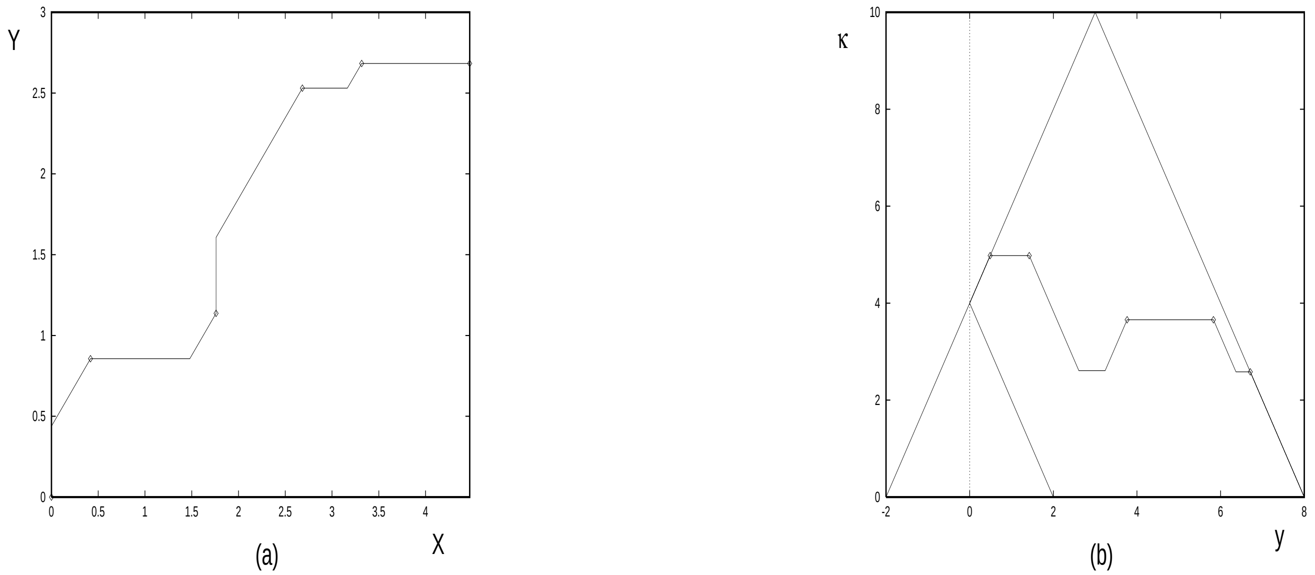

Figure 5: *An event, described in the variables (X, Y) and (y,κ), in (a) and (b) respectively.*

that the total weight for all paths, $f_0(X,Y)$, from any point (X,Y) to the end point $(0,0)$ is given by the integral over all the (ordered) (X_jY_j)-variables and the sum over all partitionings:

$$f_0(X,Y) = I_0(2\sqrt{XY}) \tag{24}$$

with I_0 the modified Besselfunction of the first kind. In order to find the weight, f_1, for all paths given the size of the parameters (a,b) we must integrate f_0 for $0 < X < a$ and $Y = b$. In this way we obtain as a first approximation to the structure function $f(x,Q^2)$ (this is straightfoward Bessel-function machinery):

$$f_1 = \sqrt{\frac{a}{b}} I_1(2\sqrt{ab}) = \frac{\partial f_0(a,b)}{\partial b} \quad \text{with} \quad \sqrt{\bar{\alpha}} f_1(a,b) \leftrightarrow \frac{\partial f}{\partial \log(Q^2)} \tag{25}$$

At the same time we conclude that the (normalized) probability to find the point (X',Y'), starting at (X,Y) is given by

$$dP(X',Y') = \frac{I_0(2\sqrt{X'Y'}) + \delta(X')\delta(Y')}{I_0(2\sqrt{XY})} dX'dY' \tag{26}$$

Given this approximate process we will now define the precise solution to the integral equation, Eq (16), for the non-integrated structure function. We will do that by introducing a weight for each particular road so that we may incorporate those features of the integral equation which are not taken into account for the solution in Eq (25). There are four such corrections and each will provide a weightfactor ρ_j so that the total weight for any road is given by $\rho = \prod_1^4 \rho_j$:

- ρ_1 The first weight is either $\rho_1 = 1$ or $\rho_1 = 0$ depending upon whether the road stays inside the "right" triangular phase space, ie whether all parts of the road is above $\kappa = 0$ or if any part is below that line, respectively.

- ρ_2 The second weight is composed of a (possible) product of subfactors, ie every time we chose a "new" $\kappa_{j+1} \equiv \log(k_{\perp j+1}^2)$ which is smaller than the previous one, ie $\kappa_j > \kappa_{j+1}$ then there should be a factor $\exp(\kappa_{j+1} - \kappa_j)$ according to Eq (9).

ρ_3 The third factor is the weight function $h(k_{\perp j}^2/k_{\perp(j-1)}^2)$ defined in Eq (8).

ρ_4 In order to introduce a running coupling $\bar{\alpha} \propto 1/\kappa$ it is possible to introduce at every vertex a correction factor $\bar{\alpha}(\kappa)/\bar{\alpha}$ (with $\bar{\alpha}$ the constant coupling considered before). It is, however, necessary to introduce some cut-off procedure to avoid values of $\kappa \simeq 0$. In this paper we only consider the choice $\bar{\alpha}(\kappa) \propto 1/\kappa$ if $\kappa > \kappa_{cut}$ and $\bar{\alpha} = \mathit{constant}$ elsewhere but we will in future publications consider the general question of infrared stability.

The product weight we define in this way is for a typical size of the phase space on the percentage level on the average but there are some interesting fluctuations. The average level, $< \rho >$, nevertheless contains the "normalization" of the precise solution to the appoximate solution we obtained in Eq (25). The final result for the structure function is consequently

$$\frac{\partial f(x,Q^2)}{\partial \log(Q^2)} =< \rho > \sqrt{\bar{\alpha}} f_1(a,b) \tag{27}$$

Inside this scheme it is evidently possible to compute not only the contribution from "the average road" but also the fluctuations around it and in particular to construct in a Monte Carlo simulation way "any" possible road. We will come back to the results of this approximate treatment both in the last section and in future publications.

3.2 A Discrete Model

We will in this subsection consider a different approach to the integral equations in Eq (16). In this approach all integrals will be exchanged for sums over a set of discrete values. The basic ideas stem from the approximate treatment of the (time-like) QCD cascades, which are presented in Ref [8]. It turns out that the density of "effective" gluons is very low in the triangular dipole phase space. The reason is three-fold (and actually corresponds to (an extension of) the Modified Leading Log Approximation, MLLA, in QCD, [5]).

The first two reasons are that there are corrections to the bremsstrahlung emission in the triangular phase space, cf Eq (10). There is eg a spin-correlation factor, which is neglected above and there are also recoil corrections in the neighbourhood of any "hard" emission. It is easy to estimate the spin-correlation corrections and also to understand the physics behind them. It is a nice surprise that these corrections also are sufficient to take into account the recoil corrections, at least in the time-like cascades as we have shown in Ref [8].

The estimate from the spin-correlation is a distance in rapidity of $\delta y = 11/6$, which is a large number. It is, however, necessary to understand that in case there is an emission of a hard gluon, a new region in phase space is opened up. This hard gluon is split into many subjets, all with approximately the same rapidity with respect to the original main axis (the thrust axis). The subjets are separated in rapidity *along the parent gluon direction* by distances δy. They contain in their turn sub-sub-jets etc. Thus within one rapidity bin δy, as measured along the thrust axis, there can be a lot of structure.

The third reason for the discretization is related to the properties of the running coupling in QCD. In Ref [8] we have exhibited that those next-order corrections (the "dielectricity of the

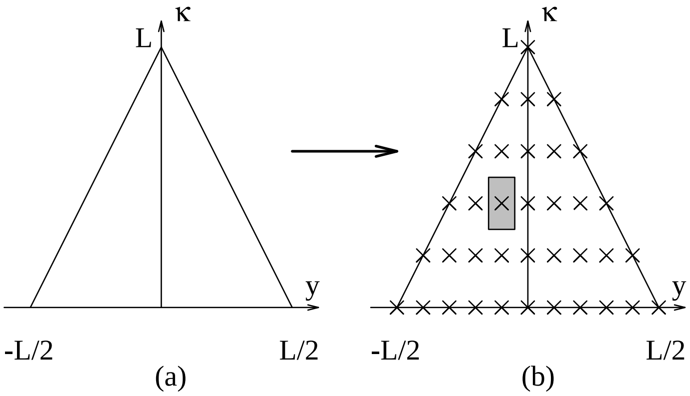

Figure 6: *(a) The continuous phase space triangle for gluon emission in* e^+e^-*-annihilation. (b) Emission points for "effective gluons" in the discretized phase space. One such gluon represents all emission that is taking place in side its cell, shaded area.*

vacuum" ie the vertex and self-energy Feynman graph corrections) which constitute the change from a constant to a running coupling actually corresponds to the requirement that if two gluons are emitted too close in rapidity then they are again reabsorbed. It turns out that it is again the same "effective" rapidity difference (as we have defined it above) of 11/6, which occurs. (We are then as before neclecting the gluon splitting process $g \rightarrow (q\bar{q})$).

Without going into the detailed arguments provided in Ref [8] we note that this number stems from the well-known formula for the effective coupling in gluon emission (with the number of flavors $N_f = 0$)

$$\bar{\alpha} \equiv \frac{N_c \alpha_s}{2\pi} = 3\frac{12\pi}{2\pi 33\kappa} = \frac{6}{11\kappa} \tag{28}$$

which will occur in the dipole emission formula according to Eq (10):

$$\bar{\alpha} d\kappa dy = \frac{6dy}{11}\frac{d\kappa}{\kappa} \tag{29}$$

From this result it is evident that with a discretization of the gluon emission rapidity steps to $\delta y = 11/6$ we obtain the (inclusive) emission density $d\kappa/\kappa$ inside each such rapidity "step". To obtain the probability to obtain a particular κ-value it is necessary to introduce a Sudakov factor. In this case the Sudakov factor becomes, [8], κ/κ_m with κ_m the largest κ-value allowed in that rapidity bin. Consequently the probability to emit an effective gluon is $d\kappa/\kappa_m$, ie it is the same for any κ-value!

We must further remember that each gluon emission corresponds to an extended phase-space fold as described in Fig 2, ie that the "extra" rapidity region obtained along the emitted gluon rapidity is given by $2\kappa/2 = \kappa$. Therefore we find in Ref [8] that it is also necessary to discretize the κ-variable into steps $\delta\kappa = 2\delta y$ in order to be able to accomodate those "collinear gluons".

The result is that the total phase space is subdivided into a set of "effective" gluon emissions and that if we discretize the rapidity region into δy-steps we are forced to discretize the corresponding κ-regions into $\delta\kappa = 2\delta y$ steps as it is shown in Fig 6. We will now introduce this same prescription into the DIS production process of dipoles.

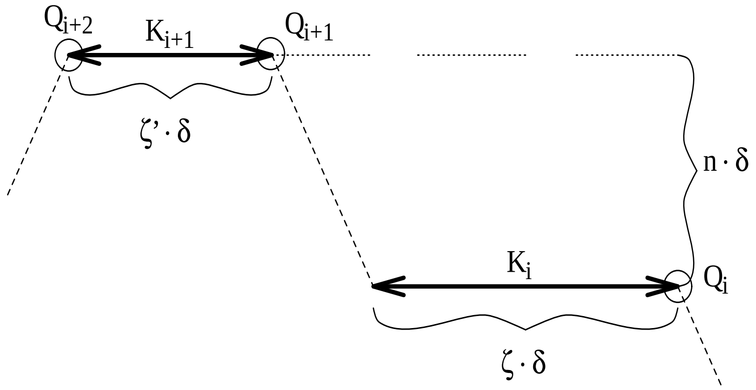

Figure 7: *Illustration of the separation conditions for propagators (arrows) and real gluons (circles) in the discretized logarithmic phase space. ζ and ζ' are integers and n is always an even integer.*

There is a small difference in the procedure, however, because the earlier argument was only related to the emission along a single original color line (a $q\bar{q}$ dipole). Although we have not been particularly precise in connection with the effective color factors it is evident that in case we consider a gluon process $g \to (gg)$ then we are actually considering a process along two color lines. It is then possible to use either the argument that there are two independently emitting color lines with the emission difference δy along each or to say that there is effectively a single emission line with the distance $\delta y/2$. We will in the spirit of the LLA keep to this latter description and therefore exchange $\delta y \to \delta y/2 \equiv \delta = 11/12$.

If we apply this scheme to the LDC Model it implies that the "links" in Fig 3 will have the property that the length of all of them is an integer times ("this new") δ and that the height is an even integer ($\neq 0$) multiplying δ. The result of a step is shown in Fig 7. This means that all real emission q-vectors will be on-shell "above" $\kappa = 0$ but it is also in this scheme possible to reach a "propagator" for which $\log(k_\perp^2)$ is zero.

The result is that inside this approach there is a finite number of chain-roads available. In each step we will obtain a weight w_i:

$$w_i = \bar{\alpha}\frac{dz_i}{z_i}d\kappa_i \equiv \bar{\alpha}2(\delta)^2\exp(n_i - \max(n_i, n_{i-1})) \tag{30}$$

For a running coupling we may write the corresponding weight

$$w_i = \frac{2}{\max(n_i, n_{i-1})}\exp\delta(n_i - \max(n_i, n_{i-1})) \tag{31}$$

The contribution from each chain is the product of all the "step-weights" and the structure function will in this scenarium be the sum over all the allowed roads (r)with their respective weights w_{ir} for each step i:

$$F(x, Q^2) = \sum_r \prod_i w_{ir} \tag{32}$$

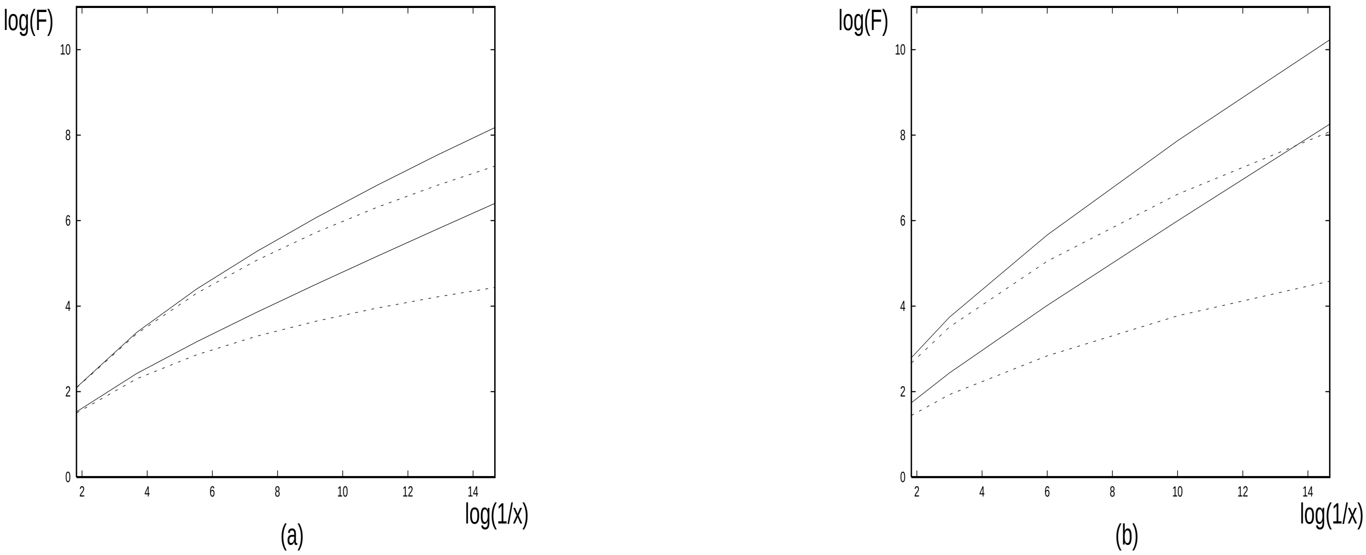

Figure 8: *The* $\log(1/x)$ *dependence for the logarithm of the structure function* $\mathcal{F}$*, when the coupling is running. Dashed lines (lower:* $\log(Q^2) \approx 4$*, upper:* $\log(Q^2) \approx 12$*) denote the DGLAP contribution and solid lines (lower:* $\log(Q^2) \approx 4$*, upper:* $\log(Q^2) \approx 12$*) all contributions. (a) The discrete model. (b) The continuous calculation.*

4 Some General Results from the LDC Model

4.1 The Behaviour of the Structure Functions

In fig 8 we show some results for the x-dependence of the structure function. It is possible to consider only the "true" DGLAP contribution to the unintegrated structure function $\mathcal{F}$, ie the case when the transverse momenta of the connector vectors are ordered, $k_{\perp 1}^2 < k_{\perp 2}^2 < ... < Q^2$. This contribution is described above by $\mathcal{I}_2$ with the same boundary value $\mathcal{I}_1$. It is shown for the two different models, according to subsections 3.2 and 3.1, in Figs 8a and 8b, respectively, as the dashed lines, corresponding to different values of $L_Q = \log(Q^2)$.

On the other hand the total integral equation solution, also including $\mathcal{I}_j, j = 3, 4$ is shown as full lines in each of the plots. There is evidently no large differences between the results from the two methods for the DGLAP contribution, but there are noticable differences in case we include the terms $\mathcal{I}_j, j = 3, 4$ both in shape and in normalization. In order to see the difference between a running and fixed coupling we show in Fig 9 a few examples for the total $\mathcal{F}$. In this case we find just as expected essential differences. The results presented here are similar to the corresponding results in ref [9] obtained in the CCFM formalism.

In Figs 10a and b we show the main path, as described by the average value of the $\kappa = \log(k_\perp^2)$ (for fixed y) for the connector vectors, from the starting-point to the final point for a "small" and a "large" value of L_Q. (We are from now on considering the total $\mathcal{F}$). We also show in the same triangular phase space the values of the connector κ-values (for fixed rapidity), which are one standard deviation above and below the average path. In both cases we have used the continuous approximation to the integral equation and a running coupling as described in subsection 3.1. In Fig 11 we show the corresponding density of emitted gluon $\log(q_\perp^2)$, this time

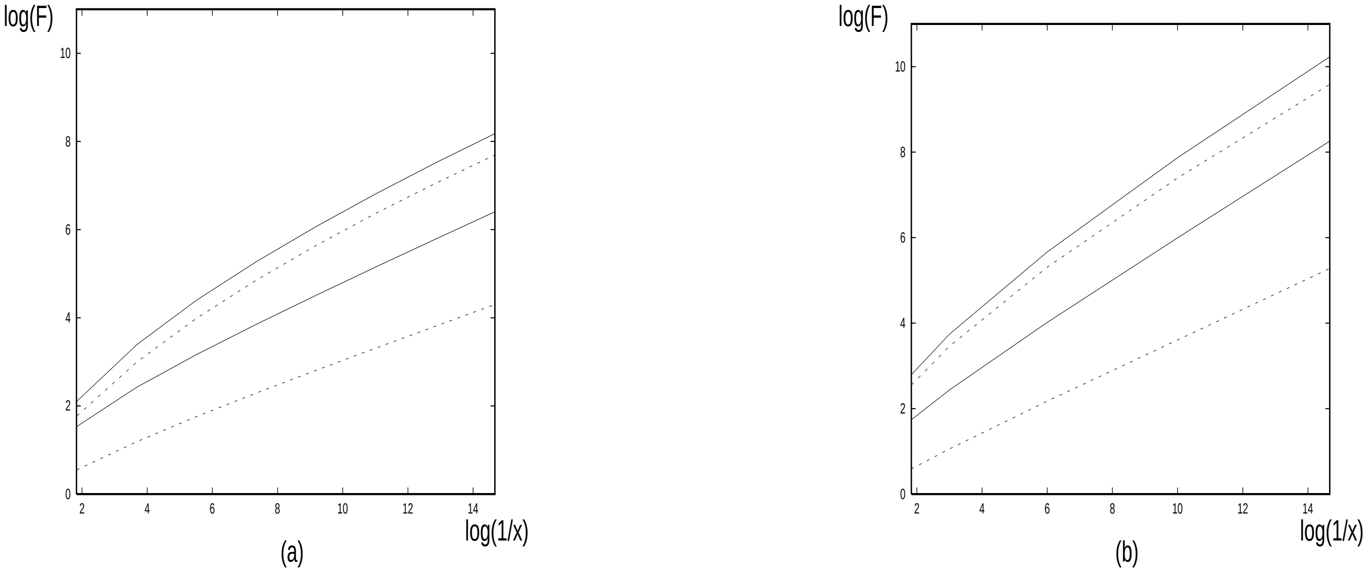

Figure 9: *The* $\log(1/x)$ *dependence for the logarithm of the structure function* $\mathcal{F}$*, when all contributions are included. Dashed lines (lower:* $\log(Q^2) \approx 4$*, upper:* $\log(Q^2) \approx 12$*) denote the result for constant coupling and solid lines (lower:* $\log(Q^2) \approx 4$*, upper:* $\log(Q^2) \approx 12$ *) denote running coupling. (a) The discrete model. (b) The continuous calculation.*

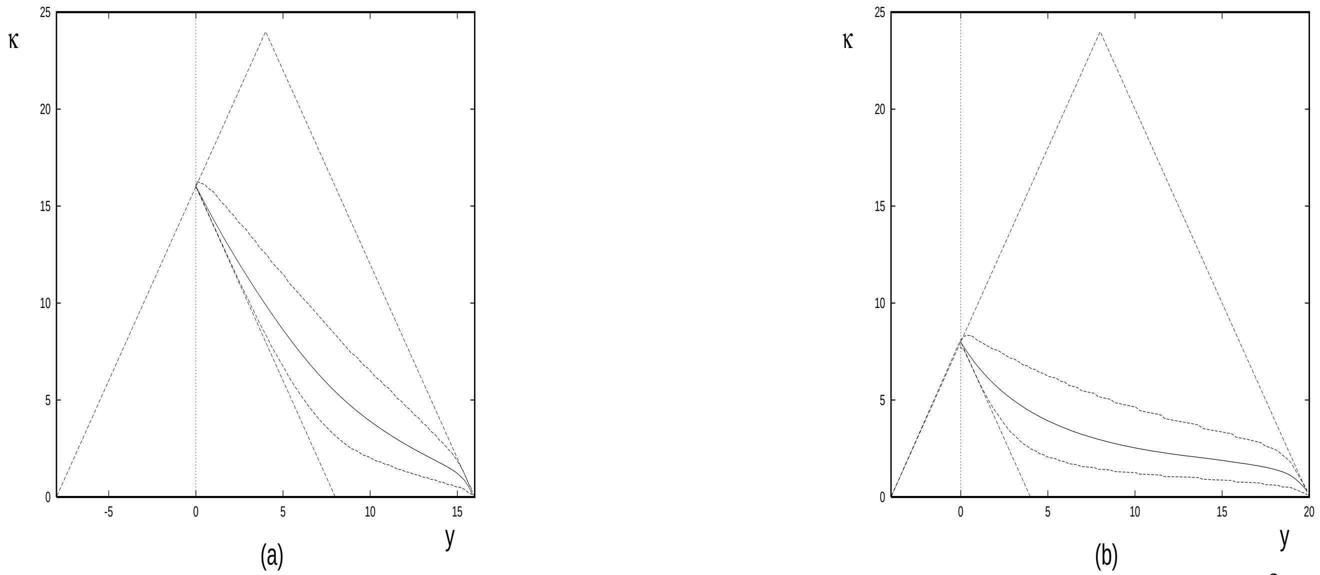

Figure 10: *The mean path and deviations from it, described in the phase space for (a)* $\log(Q^2) = 16$, $\log(1/x) = 8$ *and (b)* $\log(Q^2) = 8$, $\log(1/x) = 16$

both for a fixed and a running coupling.

We conclude from the main path-contributions that (besides a (small) $\ell = \log(1/x)$-region, ℓ_0, close to $\ell = 0$, which depends upon the way we "start out") the results can be described so that there is firstly a region ℓ_1 in which there is basically a small κ for all emissions. This corresponds to a "going-up and going-down" in a narrow region around $\kappa \simeq L_{Q0} = 0$. This is particularly so for a running coupling, which favors small κ-values. At some point it is, however, necessary to "go up" in order to end on the chosen κ, and this corresponds to a region ℓ_2. Evidently the size ℓ_2 depends upon the final "height", κ. The two regions correspond to the expected behaviour for BFKL-(ℓ_1) and DGLAP-(ℓ_2)dominance, respectively, and we will now

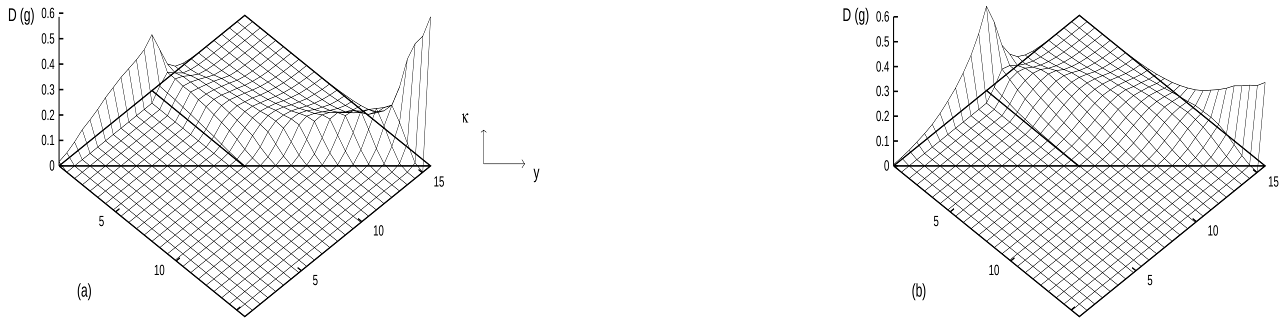

Figure 11: *The density of initial state gluons* (q_i), $D(g) = \frac{\partial^2 n}{\partial \kappa \partial y}$, *in the triangular phase space with* $\log(Q^2) = 8$ *and* $\log(1/x) = 8$. *(a): running coupling, (b): constant coupling. Inside the triangle, we have a two-dimensional distribution, while on the edges there is a one-dimensional contribution, which is sticking up.*

consider the results of an approximation, based upon such a "partitioning".

From the results of Figs 8a and 8b these conclusions are confirmed because for small values of the variable $\ell = \log(1/x)$ there is in both cases a "typical", DGLAP growth like $\log(\mathcal{F}) \simeq 2C(k_\perp^2)\sqrt{\log(1/x_B)}$ with a slow κ-dependence of the variable $C(k_\perp^2) \simeq \sqrt{\log(\kappa)}$ (valid for running α_s). (Note that inside an analytic DGLAP-approximation we obtain the behaviour $C(k_\perp^2) = \sqrt{11/12\log(\kappa)}$ for the case when we neglect n_f, the number of flavors). For larger values of ℓ, however, a basically linear behaviour of $\log(\mathcal{F})$ will dominate the amount of available paths. This is typical for the BFKL behaviour $\log(\mathcal{F}) \simeq \lambda \log(1/x)$.

The combined contribution is then (if we neglect the ℓ_0-region)

$$\mathcal{F} = \int \exp\left[2C(k_\perp^2)\sqrt{\ell_1} + \lambda \ell_2\right] d\ell_1 d\ell_2 \delta(\ell_1 + \ell_2 - \ell) \simeq \exp(\lambda \ell + [C(k_\perp^2)]^2/\lambda) \tag{33}$$

The result stems from a saddle-point approximation which is valid if the saddle point is inside the integration region, ie if $\ell_1 \equiv \tilde{\ell}_1 = [C(k_\perp^2)]^2/\lambda^2 \leq \ell$. It turns out that if we consider an approximation of the form $\log(\mathcal{F}) = a\ell + b[C(k_\perp^2)]^2 + c$, using large values of κ and ℓ from the solution to the integral equation (with $[C(k_\perp^2)]^2 \simeq \log(\kappa)$) then we always obtain results with the fitted parameters obeying $ab \simeq 1$ as expected from these considerations. The value of the λ-parameter is then $\lambda \simeq 0.4$.

On the other hand for smaller values of $\ell \leq \tilde{\ell}_1$ the DGLAP contributions will win out and dominate the results. It is possible to estimate the place where the quantity $\tilde{\ell}_1 = [C(k_\perp^2)]^2/\lambda^2 = \ell$, and rough estimates will tell us that for $x \simeq 10^{-5}$ this will occur for $Q^2 \simeq 100\ GeV^2$ (and due to the slow change of C, $x \simeq 10^{-4}$ for $Q^2 \simeq 10\ GeV^2$).

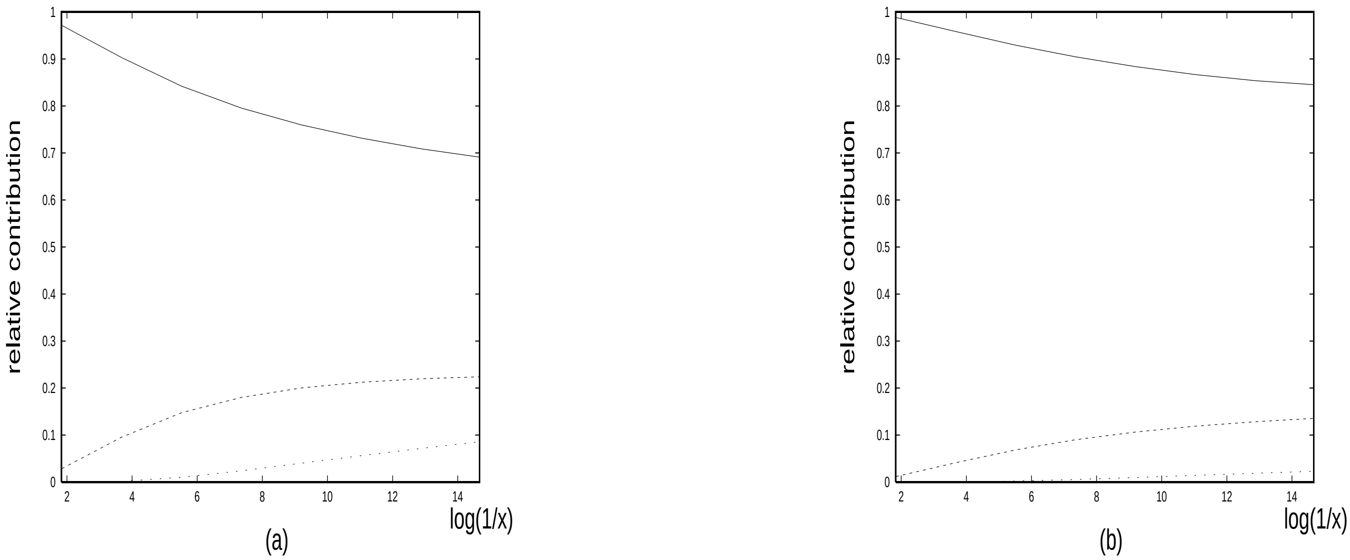

Figure 12: *The relative contributions from the different channels, determined by the discrete method. Solid lines denote Marchesini-Webber events, dashed lines boson-gluon fusion events and dotted lines Rutherford events. (a)* $\log(Q^2) = 5 \cdot \delta \approx 4.6$ *(b)* $\log(Q^2) = 9 \cdot \delta \approx 8.3$

4.2 The Contributions to the Structure Function from the Different Interaction Channels

In this subsection we would like to describe the contributions from the different channels which were described in subsection 2.3. We note in particular the boson-gluon-fusion events, which are defined so that the largest transverse momentum occurs at the last propagator link and also is larger than the momentum transfer Q. Further the Rutherford events in which one (or more) propagator links (away from the last one) have transverse momenta above Q. They correspond to hard scattering events between a resolved probe and a hadron.

The remaining events, in which no propagator transverse momenta is above Q, correspond to what we called the "normal" contribution above. (This is eg the contribution studied in ref [10] and in most situations it is the dominating term.)

In Fig 12a and b we show the contributions from these different event groups as a function of $\log(1/x)$ for two different values of $L_Q = \log(Q^2)$. We find that for a large L_Q the Marchesini-Webber events will dominate but in case we consider a small L_Q we find that the neglect of the other two groups will significantly change the result for the structure functions.

5 Summary

We have studied the behaviour of the structure function and the transverse energy flow in the Linked Dipole Chain model. In this paper we analyse only a purely gluonic cascade. In addition to a direct solution we have also studied a discretized version of the model. The result interpolates smoothly between the DGLAP region, which is applicable for
$\log(1/x) \lesssim \tilde{\ell}_1 \equiv \log[\log(Q^2)]$ (This result is applicable for a running coupling, and x is the

scaling variable for the perturbative cascade only.) and the BFKL region for larger values of $\log(1/x)$. In the latter case there is first one part of the cascade with length $\log(1/x) - \tilde{\ell}_1$, in which the transverse momenta are limited. This region is followed by a region of length $\tilde{\ell}_1$ in which the transverse momenta are growing towards the virtuality of the probe, Q. We finally study the separation of the events into normal events (where all transverse momenta are smaller than Q), boson-gluon fusion events and hard resolved photon-hadron scattering events.

Acknowledgements

This work is supported in part by the EU Programme "Human Capital and Mobility", Network "Physics at High Energy Colliders", contract CHRX-CT93-0357 (DG 12 COMA).

References

[1] B. Andersson, G. Gustafson and J. Samuelsson, Lund preprint, LU-TP 95-13

[2] M. Ciafaloni, Nucl. Phys. B296 (1988) 49
S. Catani, F. Fiorani and G. Marchesini, Phys. Lett. B234 (1990) 339; Nucl. Phys. B336 (1990) 18

[3] L. Lönnblad, Comput. Phys. Commun. 71 (1992) 15

[4] T. Sjöstrand, M. Bengtsson, Comp. Phys. Comm. 43 (1987) 367
T. Sjöstrand, JETSET 7.4, program and manual

[5] For a review, see Yu.L. Dokshitzer, V.A. Khoze, A.H. Mueller and S.I. Troyan, Basics of Perturbative QCD (Editions Frontières, Gif-sur-Yvette, 1991)

[6] B. Andersson, G. Gustafson and C. Sjögren, Nucl. Phys. B380 (1992) 391

[7] B. Andersson, G. Gustafson and Hong Pi, Z.Phys. C57 (1993) 485

[8] B. Andersson, G. Gustafson and J. Samuelsson, Lund preprint, LU-TP 95-12

[9] J. Kwieciński, A.D. Martin and P.J. Sutton, Durham preprint, DTP/95/22

[10] G. Marchesini and B.R. Webber, Nucl. Phys. B238 (1984) 1;
B.R. Webber, Nucl. Phys. B238 (1984) 492